[10] O. C. Deale, K. T. Ng, E. J. Kim-Van Housen, and B. B. Lerman, "Calibrated single-plunge bipolar electrode array for mapping myocardial vector fields in three dimensions during high-voltage transthoracic defibrillation," *IEEE Trans. Biomed. Eng.*, vol. 48, no. 8, pp. 898–910, Aug. 2001.
[11] V. Krasteva, F. A. Hatib, E. Trendafilova, and I. Daskalov, "Possibilities for predictive measurement of the transthoracic impedance in defibrillation," *J. Med. Eng. Technol.*, vol. 25, pp. 195–200, Sep.-Oct. 2001.
[12] O. C. Deale, K. T. Ng, E. J. Kim-Van Housen, and B. B. Lerman, "Simplified calibration of single-plunge bipolar electrode array for field measurement during defibrillation," *IEEE Trans. Biomed. Eng.*, vol. 49, no. 10, pp. 1211–1214, Oct. 2002.
[13] O. C. Deale, R. C. Wesley, D. Morgan, and B. B. Lerman, "Nature of defibrillation: determinism versus probabilism," *Am. J. Physiol.*, vol. 259, pp. H1544–H1550, 1990.

Wavelet-Based Cascaded Adaptive Filter for Removing Baseline Drift in Pulse Waveforms

Lisheng Xu, David Zhang*, and Kuanquan Wang

***Abstract*—This paper presents an energy ratio-based method and a wavelet-based cascaded adaptive filter (CAF) for detecting and removing baseline drift from pulse waveforms. Experiments on 50 simulated and five hundred real pulse signals demonstrate that this CAF outperforms traditional filters both in removing baseline drift and in preserving the diagnostic information of pulse waveforms.**

***Index Terms*—Baseline drift, filter, pulse waveform.**

I. Introduction

A. Pulse Waveform Analysis

Various civilizations have used arterial pulses as a guide to the diagnosis of diseases [1], [2]. Traditional chinese pulse diagnosis (TCPD) is one of the more venerable of these methodologies, boasting more than 2000 years of validated practice. All pulse diagnosis methods require that practitioners have considerable training and experience, yet even the diagnoses of practitioners with considerable experience are not always accurate. The application of pulse waveform analysis, which uses pulse sensors to quantify and analyze pulse waveforms, has the potential to be of value to all practitioners of these methods, as it has the ability to render more accurate pulse diagnoses [3]. Pulse waveform analysis is used for a variety of pathological, physiological purposes in both TCPD and Western medicine [4], [5]. However, like other physiological signals such as electrocardiograms and impedance cardiograms, pulse waveforms suffer from the subject-derived distortion known as pulse baseline drift, which arises from a subject's movement and respiration. The removal of pulse baseline drift is important to pulse waveform analyses whether they are based on Chinese or Western medical theories.

B. Related Work on Baseline Drift Removal

A number of methods have been applied to the removal of baseline drift from physiological signals, but to date all have been flawed. Polynomial interpolation, for example, is dependent on the accuracy of the detection of "knots" and may degrade as the "knots" separate. Mathematical morphology filters have also been used to remove baseline drift, but this approach requires choosing a structuring element sequence that depends on the heart rate and the shape of the physiological signal [6]. Time invariant filters have also been used to reduce baseline drift but they only attenuated baseline drift a little. Sörnmo *et al.* [7] used a time-varying filter but their approach was complex and depended on the accurate calculation of the heart rate. Similarly, adaptive filters and Wiener filters have been of limited value in the absence of prior knowledge of the physiological signal and its baseline drift [8], [9]. Our proposed wavelet-based cascaded adaptive filter (CAF) responds to all of these issues because it does not require any reference input and because the level of the baseline drift can be evaluated simply by referring the energy ratio of the pulse to its baseline drift.

II. The Proposed Cascaded Adaptive Filter

Fig. 1 depicts the proposed CAF filter. First, we decompose the pulse signal and detect its baseline drift level by computing its energy ratio (*ER*) [10]. If the *ER* is less than 50 dB, the pulse is filtered in two stages, with a discrete Meyer wavelet filter followed by cubic spline estimation. Otherwise, the pulse will be filtered using only cubic spline estimation.

A. Baseline Drift Level Detection Using Energy Ratio

When the baseline drift level is low, the frequency of the wavelet filter may be nonideal and this may introduce some distortion. To evaluate the distortion level, we propose the *ER*-based method. In wavelet analysis, a signal is split into two parts: approximation and detailed content. The approximation is then split into a second-level approximation and further details. This process can be repeated. In this paper, we use the discrete Meyer wavelet to decompose the raw pulse signal into six levels, and then compute the *ER* as

$$ER = 20\log_{10}\frac{\|A1 - \mathrm{mean}(A1)\|}{\|A6 - \mathrm{mean}(A6)\|} \tag{1}$$

where $A1$ and $A6$ are the first and the sixth level approximations of a corrupted pulse signal with $A1$ being the pulse signal and $A6$ being its baseline drift; $\|\|$ means the 2-norm and $\mathrm{mean}(A1)$ stands for the average of $A1$.

Experiments have shown that $ER = 50$ dB is the best criterion for discerning whether to use the Meyer wavelet filter. Our pulse database contains 5395 clinical pulse waveforms. These are oriented to quantify TCPD. Having calculated the *ER*s of all the pulses in this database, we find that the *ERs* of 8% of the real pulses are more than 50 dB and the *ERs* of 1.5% of the real pulses are less than 10 dB.

B. The Discrete Meyer Wavelet Filter

When the *ER* of a pulse waveform is less than 50 dB, we apply the joint time-frequency character of wavelets to remove the excessive baseline drift. We chose the discrete Meyer wavelet for this purpose because it is infinitely differentiable and can decrease to zero faster than any inverse polynomial. Moreover, it does not produce aliasing errors or distortions.

Manuscript received August 4, 2004; revised February 27, 2005. This work is supported in part by National Natural Science Foundation of China under Project 90209020 and Central/Departmental Fund of Hong Kong Polytechnic University and in part by the National Natural Science Foundation of China (NSFC)/High -Tech 863 Fund and The Departmental Fund of Hong Kong Polytechnic University. *Asterisk indicates corresponding author.*

L. Xu is with the Department of Computer Science and Technology, Harbin Institute of Technology, Harbin 150001, China (e-mail: xulisheng@ hit.edu.cn).
*D. Zhang is with the Department of Computing, Hong Kong Polytechnic University, Kowloon, Hong Kong (e-mail: csdzhang@comp.polyu.edu.hk).
K. Wang is with the Department of Computer Science and Technology, Harbin Institute of Technology, Harbin 150001, China (e-mail: wangkq@ hit.edu.cn).

Digital Object Identifier 10.1109/TBME.2005.856296

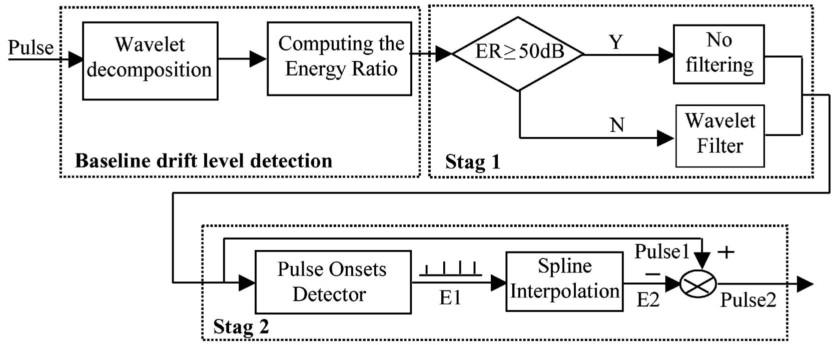

Fig. 1. The cascaded adaptive filter, which is composed of three parts: baseline drift level detection, Stag1, and Stag2. Level detection of baseline drift includes wavelet decomposition and *ER*calculation. In Stag1, if the *ER* of a pulse waveform is less than 50 dB, the wavelet filter is used. Stag2 is composed of pulse onsets detector and cubic spline estimation.

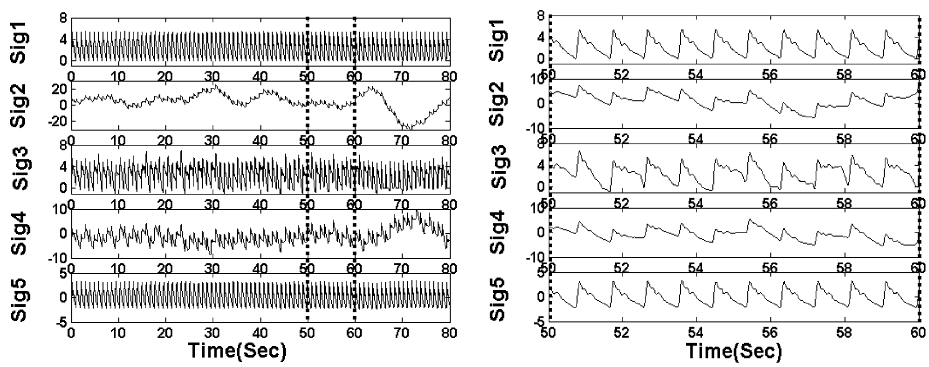

(a) (b)

Fig. 2. Performances of four filters in removing the baseline drift of pulse waveform. Fig. 2(b) is the local enlargement of Fig. 2(a). *Sig2* is attained by adding baseline drift to a clean pulse waveform *Sig1*; *Sig3*, *Sig4*, and *Sig5* are the results of *Sig2* filtered using morphological filter, FIRLS filter, and discrete Meyer wavelet filter, respectively.

We now compare the performance of the discrete Meyer wavelet filter with that of three typical filters: the morphology, finite-impulde response(FIR), and Meyer wavelet filters, excluding four other filters from the comparison. We exclude the adaptive least mean square filter and the Wiener filter because they are not sufficiently effective in removing the baseline drift from a pulse waveform when they lack a reference signal. We exclude the cubic spline method because it assumes that the *ER* of a corrupted pulse waveform is high enough. Finally, we exclude the time-varied filter proposed by Sörnmo *et al.* because it is rhythm-dependent.

As shown in Fig. 2, *Sig2* is obtained by adding baseline drift to clean pulse *Sig1*. *Sig3* is the result of *Sig2* processed by the morphological filter. We choose a disk shaped sequence with a width of 50 sampling points as the optimal structuring element sequence of this morphology filter. *Sig4* shows the result of the traditional linear-phase, least-squares-error FIR filter (FIRLS), which is a 600-order forward and reverse filter with a cutoff frequency of 0.6 Hz. *Sig5* shows the result of the discrete Meyer wavelet.

Fig. 2(b) is the local enlargement of Fig. 2(a). Compared with *Sig1*, *Sig3* is greatly distorted and *Sig4* still contains a lot of baseline drift. The Discrete Meyer wavelet filter is better than the morphological filter and the FIRLS filter both in removing *Sig2*'s baseline drift and in preserving *Sig1*'s complex. However, *Sig5* still contains some baseline drift. Note also that because the Meyer wavelet filter has enhanced the pulse waveform, spline estimation can be effectively applied to further correct the baseline drift.

C. Cubic Spline Estimation Filter

Cubic spline estimation has been chosen because when the *ER* of the pulse waveform is high, cubic spline is most suitable for estimating a baseline drift that is smooth, with at most one inflexion in every interval between adjacent knots. We regard the onsets of pulse waveform as the knots of spline estimation. An onset is defined as the starting point of the ascending part in every period of a pulse waveform, as illustrated in Fig. 3. When the *ER* and signal-to-noise ratio (SNR) of a pulse waveform are high, it is easy to accurately locate the onsets of a pulse waveform, as the onsets can be detected according to the waveform's amplitude and derivatives. Tests on 2000 clinical data and 1000 simulated pulse waveforms have shown that when $ER > 10$ dB and $\mathrm{SNR} > 15$ dB, the onsets of pulse waveforms can be detected very accurately. The accurate detection of pulse waveform's onsets ensures the accurate correction of pulse baseline drift.

III. Experimental Results

In this section, we use the same four filters in Section II-B, CAF, morphology, FIRLS filter, and spline estimation, to filter simulated signals. Baseline drift caused by respiration is simulated using a periodic component. Baseline drift caused by motion artifact is simulated using a nonperiodic component. The contaminated signals can be modeled as

$$cp(n) = p(n) + bw(n), \tag{2}$$

where $cp(n)$ is the corrupted pulse signal; $p(n)$ is a clean pulse selected from our pulse database; and $bw(n)$ is an integration of the periodic and nonperiodic parts of the baseline drift, as illustrated in (3)

$$\begin{aligned} bw(n) = a \times [&\sin(2\pi \times 0.1 \times n) + \sin(2\pi \times 0.2 \times n) \\ &+ \sin(2\pi \times 0.4 \times n) + \sin(2\pi \times 0.6 \times n) + \mathrm{filteredRandom}(n)] \end{aligned} \tag{3}$$

TABLE I
REMOVAL OF BASELINE DRIFT INTEGRATED BY PERIODIC AND NON-PERIODIC CONTENTS AT DIFFERENT ERs USING THE CUBIC SPLINE, FIRLS, MORPHOLOGY, AND CAF FILTERS

ER (dB)	*PDR*				*BCR*			
	Spline	*FIRLS*	*Morph*	*CAF*	*Spline*	*FIRLS*	*Morph*	*CAF*
40	0.002	0.002	0.015	0.001	0.04	0.05	112.78	0.011
30	0.004	0.006	0.019	0.001	0.05	0.04	10.95	0.005
20	0.011	0.015	0.021	0.001	0.06	0.04	1.25	0.003
10	0.032	0.019	0.052	0.001	0.21	0.05	0.39	0.002
5	0.117	0.051	0.073	0.001	0.22	0.05	0.23	0.002
0	0.284	0.159	0.127	0.001	0.23	0.05	0.15	0.002
-5	0.532	0.446	0.204	0.002	0.26	0.07	0.09	0.002

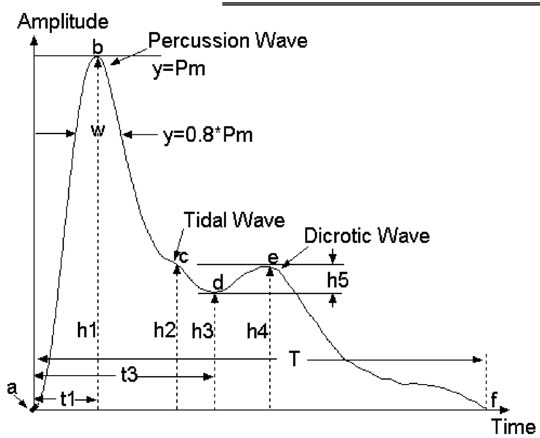

Fig. 3. Pulse and its features. A pulse waveform is usually composed of a percussion wave, tidal wave and dicrotic wave. From these waves, we extract parameters for pulse pattern recognition, where $h1$, $h2$, $h3$, $h4$, $h5$, w, $t1$, $t2$, $t3$ are the parameters, and *a*, *b*, *c*, *d*, *e*, *f* are the character points of pulse. Point "*a*" is the pulse waveform onset. If baseline drift is present, these parameters and feature points will be distorted.

where a is the amplitude coefficient of a simulated baseline. The periodic component is modeled by a sine signal at the frequency of 0.1, 0.2, 0.4, and 0.6 Hz. The nonperiodic component, $\mathrm{filteredRandom}(n)$, is modeled by the low pass filtered random noise at the cutoff frequency of 0.68 Hz.

The four filters are evaluated according to two parameters: the baseline correction ratio (BCR) and the pulse distortion ratio (PDR). These are defined as

$$\mathrm{BCR} = \frac{\sum_{t=1}^{T} \|bw(t) - bw_0(t)\|}{\sum_{t=1}^{T} \|bw_0(t)\|} \tag{4}$$

$$\mathrm{PDR} = \frac{\sum_{t=1}^{T} \|p_0(t) - p(t)\|}{\sum_{t=1}^{T} \|p_0(t)\|} \tag{5}$$

where $\|\|$ stands for 2-norm; $t \in [1, T]$, T is the length of the discrete signal; $bw_0(t)$ is the simulated baseline drift; $bw(t)$ is the baseline drift estimated by filters; $p_0(t)$ is the simulated clean pulse; and $p(t)$ is the extracted pulse.

Table I shows how the filters perform when the baseline is simulated as (2) and (3) at various *ERs*. The CAF filter has the lowest PDRs and BCRs, demonstrating that our CAF filter provides a better tradeoff between the preservation of diagnostic information and the removal of baseline drift. The morphology filter has much higher PDRs and BCRs when the *ER* is more than 20 dB, but reducing the *ER* quickly produces lower PDRs and BCRs. Cubic spline has lower PDRs and BCRs when the *ER* increases.

Our CAF filter was also tested on actual records using visual observation of three experts in TCPD. In this test, 500 clinic pulse data were randomly chosen from our pulse database and filtered using our CAF filter. Three experts in TCPD were then asked first to diagnose through analyzing these 500 raw pulse waveforms, and then their 500 processed pulse waveforms. After CAF filtering, the accuracy of diagnosis rose from 67% to 83%, demonstrating the effectiveness of the CAF filter.

IV. CONCLUSION

This CAF filter efficiently and robustly corrects baseline drift in pulse waveforms, making it very useful in preprocessing pulse waveforms based on both TCPD and Western medicine. The results suggest that this CAF filter could also be used to remove baseline drift from other physiological signals.

ACKNOWLEDGMENT

The authors would like to thank all of the volunteers for providing the invaluable pulse data.

REFERENCES

[1] S. Z. Li, *Pulse Diagnosis*. Kent, WA: Paradigm, 1985.
[2] R. B. Amber, *Pulse Diagnosis: Detailed Interpretations for Eastern & Western Holistic Treatments*. London, U.K.: Aurora, 1993.
[3] W. A. Lu, Y. Y. Wang, and W. K. Wang, "Pulse analysis of patients with severe liver problems," *IEEE Eng. Med. Biol. Mag.*, vol. 18, no. 1, pp. 73–75, Jan.-Feb. 1999.
[4] Y. Z. Yoon, M. H. Lee, and K. S. Soh, "Pulse type classification by varying contact pressure," *IEEE Eng. Med. Biol. Mag.*, pp. 106–110 , Nov./Dec. 2000.
[5] A. N. Michael, J. B. Carolyn, A. H. Geoffrey, H. R. James, and C. M. Simon, "A real-time algorithm for the quantification of blood pressure waveforms," *IEEE Trans. Biomed. Eng.*, vol. 49, no. 7, pp. 662–670, Jul. 2002.
[6] Y. Sun, K. L. Chan, and S. M. Krishnan, "ECG signal conditioning by morphological filtering," *Comput. Biol. Med.*, vol. 32, pp. 465–479, 2002.
[7] Sörnmo, "Time-varying filtering for removal of baseline wander in exercise ECGs," in *Proc. Computers in Cardiology*, 1991, pp. 145–148.
[8] N. V. Thakor and Y. S. Zhu, "Application of adaptive filtering to ECG analysis: Noise cancellation and arrhythmia detection," *IEEE Trans. Biomed. Eng.*, vol. 38, no. 8, pp. 785–794, Aug. 1991.
[9] C. C. Chiu and S. J. Yeh, "A tentative approach based on Wiener filter for the reduction of respiratory effect in pulse signals," in *Proc. 19th Int. Conf. IEEE/EMBS*, Oct. 1997, pp. 1394–1397.
[10] K. Q. Wang and L. S. Xu, "Pulse baseline wander removal using wavelet approximation," in *Proc. Computers in Cardiology*, 2003, pp. 605–608.